Study on gamma response function of EJ301 organic liquid scintillator with GEANT4 and FLUKA *

ZHANG Su-Ya-La-Tu(张苏雅拉吐)[1,2] CHEN Zhi-Qiang(陈志强)[1;1)] HAN Rui(韩瑞)[1,4]
LIU Xing-Quan(刘星泉)[1,2] R.Wada[1,3] LIN Wei-Ping(林炜平)[1,2] JIN Zeng-Xue(靳增雪)[1,2]
XI Yin-Yin(席印印)[5] LIU Jian-Li(刘建立)[1] SHI Fu-Dong(石福东)[1]

[1] Institute of Modern Physics, Chinese Academy of Sciences, Lanzhou 730000, China
[2] University of Chinese Academy of Sciences, Beijing 100049, China
[3] Cyclotron Institute, Texas A&M University, College Station, Texas 77843, USA
[4] Lanzhou University, Lanzhou 730000, China
[5] College of Nuclear Science and Technology, Harbin Engineering University, Harbin 150000, China

Abstract: The gamma response function is required for energy calibration of EJ301 (5 cm in diameter and 20 cm in height) organic liquid scintillator detector by means of gamma sources. The GEANT4 and FLUKA Monte Carlo simulation packages were used to simulate the response function of the detector for standard ^{22}Na, ^{60}Co, ^{137}Cs gamma sources. The simulated results showed a good agreement with experimental data by incorporating the energy resolution function to simulation codes. The energy resolution and the position of the maximum Compton electron energy were obtained by comparing measured light output distribution with simulated one. The energy resolution of the detector varied from 21.2% to 12.4% for electrons in the energy region from 0.341 MeV to 1.12 MeV. The accurate position of the maximum Compton electron energy was determined at the position 81% of maximum height of Compton edges distribution. In addition, the relation of the electron energy calibration and the effective neutron detection thresholds were described in detail. The present results indicated that both packages were suited for studying the gamma response function of EJ301 detector.

Key words: gamma response function, EJ301 organic liquid scintillator, energy calibration, energy resolution function, GEANT4, FLUKA, Compton edge

PACS: 29.40.Mc, 24.10.Lx, 07.85.-m **DOI:** 10.1088/1674-1137/37/12/126003

1 Introduction

Organic liquid scintillator EJ301 (equivalent to BC501A, NE213) is widely used in many nuclear physics studies involving neutrons, because of its superior time resolution, excellent n-γ discrimination properties and high neutron detection efficiency. The response of an organic liquid scintillator [1, 2] is dependent upon the specific ionization of the detected particles. The gamma rays and neutrons can be detected by producing recoil electrons or recoil nuclei within the scintillator material. The response of the organic liquid scintillator to particle energies is nonlinear except for electrons. The electron energy calibration of the organic liquid scintillator detector with standard gamma sources [3–6] is very important not only for estimation of effective neutron detection thresholds and determining the accurate neutron detection efficiency, but also for unfolding the measured pulse height spectrum. There are different methods [3–11] for how to associate measured pulse height spectrum with energies by using standard gamma sources. A typical method is the threshold to be evaluated from the peak energy and the Compton edge of standard gamma source. However these positions depend on the detector characteristics, such as energy resolution. In many applications, these characteristics are ignored and the results are different even for similar detectors. It has been shown that the most convenient and useful method is given by the Monte Carlo method in which the position of the Compton edge is precisely determined by comparing a measured with a calculated one. The accuracy of any Monte Carlo simulation must be accompanied by validation of the codes against experimental data, and by comparison between different packages. The GEANT4 [12, 13] and FLUKA [14, 15] are well-established Monte Carlo simulation packages in nuclear and particle physics, and

Received 01 March 2013
∗ Supported by National Natural Science Foundation of China (11075189), 100 Persons Project (0910020BR0, Y010110BR0) and ADS Project 302 (XDA03030200) of the Chinese Academy of Sciences
1) E-mail: zqchen@impcas.ac.cn

can be used to simulate the response function and the efficiency of detector [16–18].

In this paper, the light output of EJ301 organic liquid scintillator detector for standard gamma sources was simulated by GEANT4 and FLUKA Monte Carlo simulation packages and folded properly with the energy resolution function of the detector. The simulated results were compared with experimental data for standard ^{22}Na, ^{60}Co, ^{137}Cs gamma sources. The energy resolution of the detector and the accurate position of the maximum Compton electron energy were obtained by comparing measured light output distribution with simulated results. The method of electron energy calibration of EJ301 detector by means of gamma rays was described in detail. In addition, the relation of the electron energy calibration and the effective neutron detection thresholds of the detector will be discussed.

2 Experiment

In the present work, the gamma response functions of EJ301 organic liquid scintillator were measured with standard ^{22}Na, ^{60}Co and ^{137}Cs gamma sources. The purpose of the experiment was to relate light output distribution to the actual energy loss to the integrated charge measured by the photo-multiplier pulses, using the Compton edges. Standard gamma sources were mounted on the center of the entrance window of a cylindrical (5 cm in diameter and 20 cm in height) EJ301 scintillator. The gamma rays emitted from source were detected by EJ301 scintillator coupled to an ET 9813KB photo-multiplier tube(PMT).

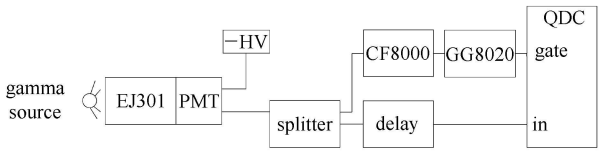

Fig. 1. Experimental setup and electronics setup of gamma response measurement.

The layout of experimental setup and electronics setup are shown in Fig. 1. The anode pulses from the PMT of the EJ301 neutron detector were branched into two by signal dividers. The electronic charges of the one branch were recorded by the Phillips 7166 QDC. The other one was sent to ORTEC CF8000 (constant fraction discriminator) and ORTEC GG8020 (gate generator) for a common gate of QDC. The light output data was collected on an event-by-event basis using a CAMAC-based online data acquisition system. The light output distributions of standard ^{22}Na, ^{60}Co and ^{137}Cs gamma sources were obtained. Background was measured and extracted in the offline data analysis.

Data analysis was done using the ROOT packages developed at CERN, which was an object-oriented framework used worldwide for data analysis.

3 Simulation

The gamma response functions of EJ301 (5 cm in diameter, 20 cm in height) organic liquid scintillator detector with standard ^{22}Na, ^{60}Co and ^{137}Cs gamma sources have been studied with GEANT4.9.5 and FLUKA-2011 Monte Carlo simulation packages. In this simulation, a simple model of the detector was used for the EJ301 organic liquid scintillator with Al-capsules. Material components of the EJ301 scintillator were H and C (ratio of atoms is 1.212, density of the scintillator is 0.874 g/cm^3). The scintillator was filled into a 5 cm in diameter and 20 cm in height cylindrical vessel with 0.5 mm thick aluminum. The light pipe and PMT were ignored.

3.1 GEANT4 Monte Carlo simulation

In this section GEANT4 simulation is described. The standard electro-magnetic physics and new data set G4EMLOW.6.23 were used in this simulation. No production thresholds were applied for electrons and positrons. All possible processes of light production inside the detector, resolution function of the detector and light response of Compton electrons were considered. The scintillation light output from the electrons was due to the gamma rays interacting with the materials of the detector. Energy deposition of electrons was recorded step by step for every event and was converted into the light output by the following formula [1, 2, 8–10]

$$L=\alpha(E_{\rm e}-E_0), \tag{1}$$

where L is the light output in MeVee, $E_{\rm e}$ is the electron energy in MeV, E_0 is a parameter due to the nonlinear relation at lower energies and α is the light output scaling parameter. $\alpha=1$ and $E_0=0$ are used in the present work.

To compare the simulated light output with the experimental data, the energy resolution function of the detector was taken into account by Gaussian-broadening on light output L with resolution width ΔL. As shown in Fig. 2, the GEANT4 simulated result is in good agreement with the respective experimental data for the standard ^{22}Na, ^{60}Co and ^{137}Cs gamma sources. In Fig. 2, the black solid circle is the experimental data, red open circle is the GEANT4 simulated result and green solid line is FLUKA simulated result.

3.2 FLUKA simulation

In this paper, FLUKA [14, 15] Monte Carlo simulated results were compared to the experimental data and the GEANT4 simulated results. FLUKA can simulate with

high accuracy the interaction and propagation in matter of about 60 different particles, including photons and electrons from 1 keV to thousands of TeV. One of the best features of FLUKA is the implementation and improvement of sound and modern physical models and it cannot be influenced by the user. Some processes and parameters such as cutoff energies can be changed by enabling or disabling the corresponding card. The card BEAM defines the particle energy (or momentum) and the card BEAMPOS defines the starting position and direction of the particle beams. These two commands can be used also to define particle beams having a simple angular or energy (or momentum) distribution (Gaussian or rectangular).

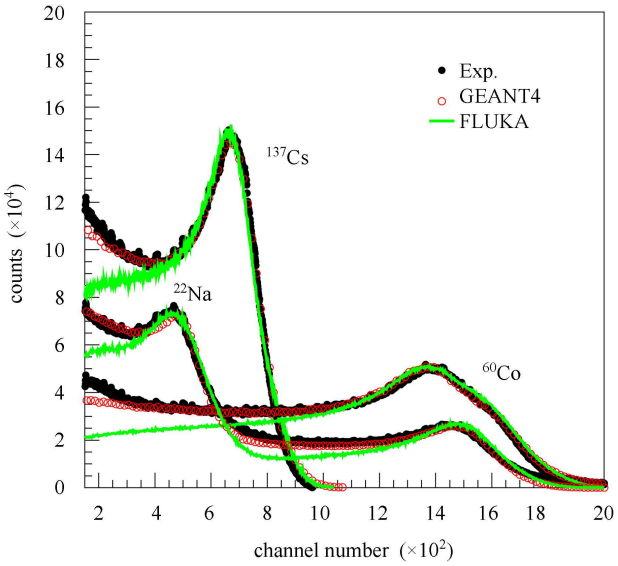

Fig. 2. (color online) Comparison of the experimental light output with the GEANT4, FLUKA simulation results. The black solid circle is the experimental data, red open circle is the GEANT4 simulated result and green solid line is the FLUKA simulated result.

The FLUKA simulation was carried out for a detailed description of an ideal experimental set-up. The detector geometry was simulated according to the characteristics discussed above. The energy resolution function of the detector was incorporated by considering a Gaussian energy spread ΔE of the beam on BEAM card. Particle energy loss was recorded by EVENTBIN card and converted into light output by Birks law [1] of the TCQUENCH card. The results of FLUKA simulation are compared with GEANT4 results and experimental data, as shown in Fig. 2. Although by comparison it is shown that results of simulation agree well with the experimental data around the Compton edge, there are some discrepancies at lower pulse-height (also mentioned in [19, 20]). These discrepancies might be caused by: (a) the effects of surrounding materials like holders are not included in FLUKA simulation code; (b) the effect of setting lower thresholds for photon and electron transport in FLUKA simulation code; (c) the edge (or wall) effect, which is not well considered in FLUKA simulation code, etc.

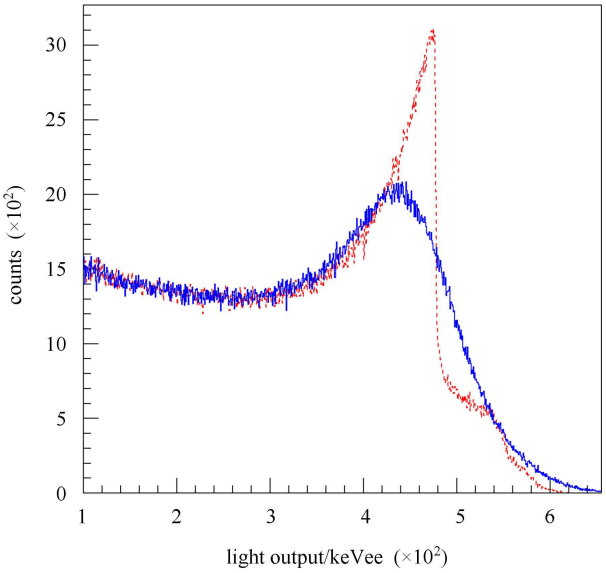

Fig. 3. (color online) Simulated Compton electron spectrum from a ^{137}Cs source (red dashed line) and the same spectrum folded with resolutions 18.1% (blue solid line).

4 Results and discussion

4.1 Energy resolution of detector

The gamma source geometry, the position of the source, the size of the detector and the detector walls, and the resolution function of the detector system strongly affected the shape of the light output distribution of the detector. The resolution function of the detector can be described by the formula [3–6, 18, 21, 22]:

$$\frac{\Delta L}{L}=\sqrt{\alpha^2+\frac{\beta^2}{L}+\frac{\gamma^2}{L^2}}. \quad (2)$$

This formula describes light output resolution of the detector due to various effects. The first term α describes the locus-dependent light transmission from the scintillator to the photocathode and limits the resolution of the detector system at high pulse heights; the statistical variation of the light production, attenuation, conversion of photon-electron and electron amplification was described by the second term β; the third term γ is due to the noise contributions from PMT (dark current) and electronic system.

The resolution parameters for any particular detector setup must be determined either experimentally by

means of mono-energetic photon and neutron sources or theoretical estimates [3]. In this work, the value of the parameters α, β, γ have been obtained by comparing the simulation spectrum of gamma sources with the respective experimental data. $\alpha = 0.05$, $\beta = 0.12$, $\gamma = 0.002$ are the best parameters for standard ^{22}Na, ^{60}Co and ^{137}Cs gamma sources. Fig. 3 shows a GEANT4 simulated Compton electron spectrum with ^{137}Cs gamma source and the same spectrum folded with the energy resolution of 18.1%. The observed large difference indicates that the simulated spectrum has to be folded with energy resolution of the detector for comparison with experimental data. In Fig. 4, relations for the energy resolution of the detector as a function of the electron energy are given. The black solid circle is the experimental data and the red solid line is the result of fitting experimental data by quartic polynomial.

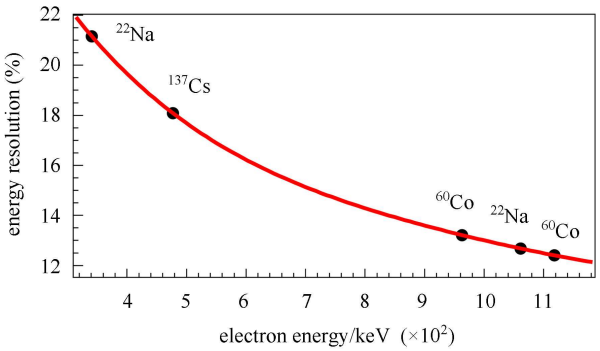

Fig. 4. (color online) Energy resolution of 5 cm diameter, 20 cm thick EJ301 organic liquid scintillator detector as a function of the electron energy. The black solid circle is the experimental data and the red solid line is the result of fitting experimental data by quartic polynomial.

4.2 Position of the Compton edge

The light output distribution of gamma rays for the organic liquid scintillator are mainly due to Compton scattered electrons, because the photo-peak cross section is very small for photon energies $E \leqslant 3$ MeV [3, 5, 6]. The maximum energy of Compton recoil electron (E_c) is determined by a theoretical formula

$$E_c = \frac{2E_\gamma}{m_e c^2 + 2E_\gamma}. \quad (3)$$

In Table 1, the position of maximum of the Compton edges energy E_{max}, half height of maximum of the Compton edges energy $E_{1/2}$ and maximum of the Compton electron energy E_c for standard ^{22}Na, ^{60}Co and ^{137}Cs gamma source is shown.

Because of the difference of experimental method, detector size and detector casing, the location of gamma source relative to the detector and the resolution of detector, different positions of the maximum energy of Compton recoil electron were reported in different papers. In the past, many authors assumed the half-height of the Compton electron distribution to be the location of maximum of Compton electron energy [3–6]. Also, many papers [3–11] have shown the results that the position of the Compton edge (E_c) occurs at 72%, 89%±7%, 75% and 66% of the Compton edges distribution. In this work, the accurate position of the Compton edges is determined by comparing measured light output distribution with simulated results. As shown in Fig. 5, the position of the Compton edge is corresponding to 81% of the maximum height of the Compton edges distribution. This result is consistent with the literature [4, 5, 8].

Table 1. E_γ, E_c, E_{max}, $E_{1/2}$ of different gamma sources.

source	E_γ/MeV	E_c/MeV	E_{max}/MeV	$E_{1/2}$/MeV
^{22}Na	0.511	0.341	0.298	0.396
^{137}Cs	0.662	0.477	0.438	0.509
^{60}Co	1.17	0.963	0.928	1.11
^{22}Na	1.27	1.06	1.01	1.11
^{60}Co	1.33	1.12	1.08	1.15

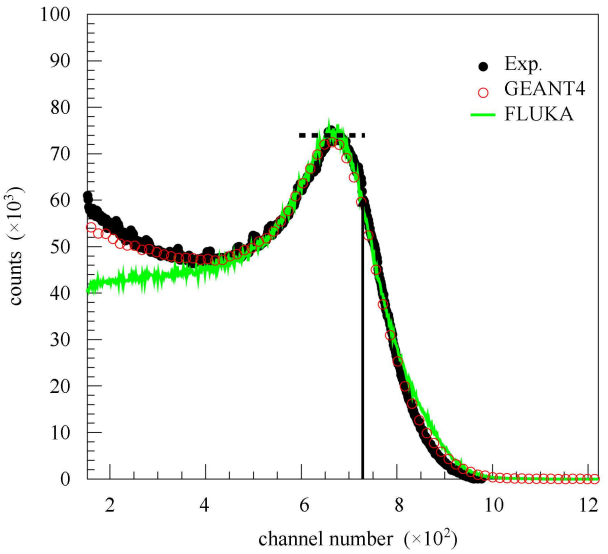

Fig. 5. (color online) The channel numbers are linearly related to the deposited electron energy through calibration points corresponding to 81% of the maximum of the Compton edges.

4.3 Energy calibration of detector

In this paper, the electron energy calibration of EJ301 organic liquid scintillator detector is obtained with relating the accurate position of the measured Compton edge to the maximum energy of the Compton recoil electron for standard ^{22}Na, ^{60}Co and ^{137}Cs gamma sources. As discussed above, the accurate position of the Compton edge is determined by comparing measured light

output distribution with simulated spectrum properly folded with the energy resolution of the detector. As shown in Fig. 6, the red solid line is the result of experimental data (the black solid circle) fitted by the first-order polynomial, it can be expressed by Eq. (4), where $b_0=0.038\pm0.046$, $b_1=1.493\pm4.058e-5$. Eq. (4) is the electron response function of EJ301 organic liquid scintillator detector. The experimental error was included in the experimental data.

$$L(E_{\rm e})=b_0+b_1E_{\rm e}. \tag{4}$$

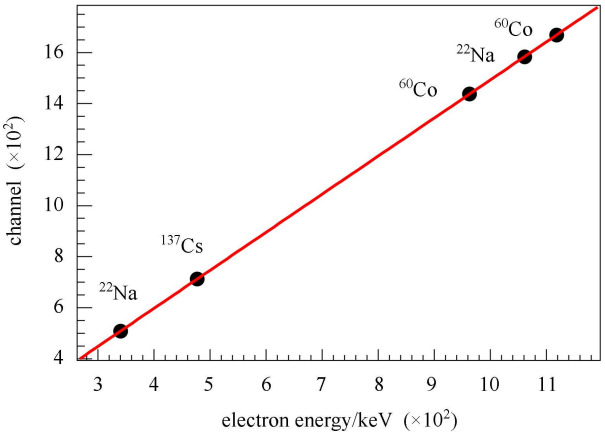

Fig. 6. (color online) Energy calibration of 5 cm diameter, 20cm thick EJ301 organic liquid scintillator detector. The red solid line is the result of experimental data (the black solid circle) fitted by the first-order polynomial.

4.4 Neutron detection threshold

In the simulation of efficiency of neutron detector, the effective neutron detection threshold (the average recoil proton energy which produces just enough light in the scintillator to be detectable at a given experimental discrimination level) must be known accurately [3, 7, 21]. It's well known that neutron detection efficiency is proportional to $(1-E_{\rm th}/E_{\rm n})$, with $E_{\rm n}$ being the neutron energy and $E_{\rm th}$ being the threshold. When neutron energy is less than $2E_{\rm th}$, the relative error of detection efficiency increases rapidly with the reduction of neutron energy. The effective neutron detection threshold of the scintillator detector can be obtained by means of electron energy calibration of the detector [3–7, 23] and taking the equivalent proton energy (the energy of protons producing the same amount of light) from the proton to electron response. The light output from the charged particles produced in the scintillator detector due to interaction of neutrons can be estimated by Birks's law [1, 24] and Cecil's description [18, 25]. In Cecil's description, the total light output for proton of energy $E_{\rm p}$ is given by Eq. (5), where $a_1=0.83$, $a_2=2.82$, $a_3=0.25$, $a_4=0.93$.

$$L(E_{\rm p})=a_1E_{\rm p}-a_2(1-{\rm e}^{-a_3E_{\rm p}^{a_4}}). \tag{5}$$

From Eqs. (4) and (5), the relation of proton response and electron response of the scintillator is obtained, as shown in Eq. (6).

$$E_{\rm e}=\frac{a_1E_{\rm p}-a_2(1-{\rm e}^{-a_3E_{\rm p}^{a_4}})-b_0}{b_1}. \tag{6}$$

For example, the total energy peak produced by the 662 keV gamma rays from a ^{137}Cs corresponds to roughly 2.44 MeV protons. This is slightly different from reference [2, 3]. Such difference is mostly because a different method of energy calibration of detector and experimental setup has been used.

5 Summary

The gamma response function of EJ301 (5 cm in diameter and 20 cm in height) organic liquid scintillator detector was simulated using GEANT4 and FLUKA Monte Carlo simulation packages and compared with the respective experimental data for the standard ^{22}Na, ^{60}Co and ^{137}Cs gamma sources. It's found that simulated results agree well with experimental data by considering the energy resolution function of the detector to simulation codes. The best resolution parameters ($\alpha=0.05$, $\beta=0.12$, $\gamma=0.002$) of the energy resolution function of the detector were obtained with ^{22}Na, ^{60}Co and ^{137}Cs gamma sources. For the electron energy calibration of the detector, the accurate position of the Compton edge was determined at the position 81% of maximum height of Compton edges distribution by comparing measured light output distribution with simulated results. As shown in Fig. 6, the light output is linearly related to the deposited electron energy for EJ301 detector. The relation of proton response and electron response was also obtained by using electron energy calibration and the proton response of Cecil's description. It indicated that the electron energy calibration of the detector has played a very important role in determination of accurate effective neutron detection thresholds. The present results verified that both packages were suited for studying the gamma response function of EJ301 detector.

References

1 Birks J B. The Theory and Particle of Scintillation Counting. London: Pergamon Press, 1964
2 Smith D L, Polk R G, Miller T G. Nucl. Instrum. Methods, 1968, **64**: 157–166
3 CHEN J X, SHI Z M, TANG G Y. Nuclear Electronics & Detection Technology, 1994, **14**: 140–147 (in Chinese)
4 YAN J, LIU R, LI C et al. Chinese Physics C (HEP & NP), 2010, **34**(7): 993–997
5 Dietze G. IEEE Trans. Nucl. Sci, 1979, **NS-26**: 398–402
6 Dietze G, Klein H. Nucl. Instrum. Methods, 1982, **193**: 549–556
7 Knox H H, Miller T G. Nucl. Instrum. Methods, 1972, **101**: 519–525
8 Flynn K F, Glendenin L E, Steinberg E P et al. Nucl. Instrum. Methods, 1964, **27**: 13
9 Prescott J R, Rupaal A S. Can. J. Phys, 1961, **39**: 221–226
10 Czirr J B, Nygren D R, Zafiratos C D. Nucl. Instrum. Methods, 1964, **31**: 226–234
11 Nardi E. Nucl. Instrum. Methods, 1971, **95**: 229–232
12 Agostinelli S, Allison J, Amako K et al. Nucl. Instrum. Methods A, 2003, **506**: 250-303
13 Allison J, Amako K, Apostolakis J et al. IEEE Trans. Nucl. Sci, 2006, **53**: 270–278
14 Ferrari A, Sala P R, Fasso A et al. CERN-2005-10, INFN/TC_05/11, SLAC-R-773, 2005
15 Battistoni G, Muraro S, Sala P R et al. AIP Conference Proceeding, 2007, **896**: 31–49
16 Patronis N, Kokkoris M, Giantsoudi D et al. Nucl. Instrum. Methods A, 2007, **578**: 351–355
17 Borio di Tiglioe A, Cesana A, Dolfini R et al. Nucl. Instrum. Methods A, 2001, **469**: 347–352
18 Gohil M, Banerjee K, Bhattacharya S et al. Nucl. Instrum. Methods A, 2012, **664**: 304–309
19 Ranjbar Kohan M, Etaati G R, Ghal-Eh N et al. Applied Radiation and Isotopes, 2012, **70**: 864–867
20 Vincke H, Gschwendtner E, Fabjan C W et al. Nucl. Intrum. Methods A, 2002, **484**: 102–110
21 Dekempeneer E, Liskien H. Nucl. Instrum. Methods A, 1987, **256**: 489
22 Litaize O. Nucl. Instrum. Methods A, 2007, **580**: 98–101
23 Franke R, Steinheuer B, Witsch W Von al. Nucl. Instrum. Methods, 1982, **198**: 311–315
24 ZHANG S, LIN W, Rodringues M R D et al. Nucl. Instrum. Methods A, 2013, **709**: 68–71
25 Cecil R A, Anderson B D, Madey R. Nucl. Instrum. Methods, 1979, **161**(3): 439–447